



## City Research Online

### City, University of London Institutional Repository

---

**Citation:** Rajana, K. & Giaralis, A. (2022). A hybrid nonlinear rooftop isolated tuned mass damper-inerter system for seismic protection of building structures. Proceedings of the International Conference on Natural Hazards and Infrastructure, ISSN 2623-4513

This is the accepted version of the paper.

This version of the publication may differ from the final published version.

---

**Permanent repository link:** <https://openaccess.city.ac.uk/id/eprint/30096/>

**Link to published version:**

**Copyright:** City Research Online aims to make research outputs of City, University of London available to a wider audience. Copyright and Moral Rights remain with the author(s) and/or copyright holders. URLs from City Research Online may be freely distributed and linked to.

**Reuse:** Copies of full items can be used for personal research or study, educational, or not-for-profit purposes without prior permission or charge. Provided that the authors, title and full bibliographic details are credited, a hyperlink and/or URL is given for the original metadata page and the content is not changed in any way.

---

---

---

City Research Online:

<http://openaccess.city.ac.uk/>

[publications@city.ac.uk](mailto:publications@city.ac.uk)

---

# A hybrid nonlinear rooftop isolated tuned mass damper-inerter system for seismic protection of building structures

Komal Rajana<sup>1</sup>, M.Sc., Agathoklis Giaralis, Ph.D., M.ASCE  
City, University of London, UK

## ABSTRACT

In recent years, the passive tuned mass damper inerter (TMDI) has been widely considered in the literature for the seismic demand mitigation of building structures. Its effectiveness relies on careful design/tuning of the TMDI stiffness and damping properties, while its performance improves with the increase of the inertance property, which is readily scalable, as well as with spanning several floors when placed to the top of buildings. Nevertheless, TMDI configurations spanning several floors may be impractical for ordinary structures. This paper addresses the above issue by presenting a novel hybrid energy dissipation system, termed rooftop isolated tuned mass damper inerter (RI-TMDI). The RI-TMDI comprises an additional seismically isolated floor with a TMDI placed atop of buildings, making it applicable for seismically retrofitting of existing structures as well as for enhancing the seismic performance of new structures. The motivation of the RI-TMDI is based on the fact that the vibration control potential of TMDIs improve as the floor they are installed to is designed to be more flexible. Herein, a three degree of freedom (3-DOF) structural system is put forward to study the potential of RI-TMDI for seismic response mitigation of buildings, modelled as linear damped single degree of freedom structures, in which isolator bearings are modelled through the Bouc-Wen model. Statistical linearization is applied to expedite optimal RI-TMDI tuning such that the input energy dissipated by the TMDI is maximized under white noise excitation. A pilot parametric numerical investigation is undertaken to assess the influence of the isolator flexibility and damping properties and of the TMDI inertance to the tuning and performance of the RI-TMDI under white noise excitation. Further, results from nonlinear response history analyses for four recorded GMs applied to optimally tuned RI-TMDI systems are reported. It is found that the efficacy of RI-TMDI for suppressing seismic structural displacement demands improves as the effective post-yielding flexibility of the isolators increases, provided that the TMDI is equipped with sufficiently high inertance. However, this improvement comes at the cost of increased deflection of the isolators. To this end, it is shown that by increasing inertance both building and isolator displacements may be reduced.

*Keywords: hybrid passive vibration control, tuned mass damper inerter, seismic isolation, optimal design*

## INTRODUCTION AND MOTIVATION

Over the past decades, the passive linear tuned mass damper (TMD) has been widely studied in the scientific literature for the seismic protection of conventional fixed-based buildings (see e.g. De Angelis et al. 2012 and references therein) as well as base isolated buildings (see e.g. De Domenico and Ricciardi 2018a and references therein). The TMD comprises a secondary free-to-oscillate mass attached to the building (primary) structure via stiffeners, commonly modelled as a linear spring, in parallel with viscous dampers, commonly modelled as a linear dashpot. The TMD stiffness and damping properties are designed/tuned for a given secondary mass to minimize the primary structure response of interest. For fixed-based buildings TMDs are typically placed to the top floor aiming to mitigate top floor dynamics by tuning to the first (fundamental) building natural period. For base isolated buildings, the TMD is placed at the isolation layer (basement) aiming to mitigate the lateral sway of the isolators.

Regardless of the TMD placement and the type of primary building structure, TMDs require significantly large secondary mass for the effective mitigation of earthquake-induced oscillations (De Angelis et al 2012,

---

<sup>1</sup> Corresponding Author: Komal Rajana, Ph.D. Candidate. E-mail: [komal.rajana@city.ac.uk](mailto:komal.rajana@city.ac.uk)

Reggio and De Angelis 2015). To relax this requirement, Marian and Giaralis (2013, 2014) introduced the tuned mass damper inerter (TMDI) configuration which couples the TMD with an inerter, a mechanical device that produces a resisting force proportional to the relative acceleration at its ends (Smith 2002). The device constant of proportionality is termed ‘inertance’ and is in mass units (kg). In the TMDI, the inerter acts as a mass amplifier contributing inertia (but not weight) to the TMD through the inertance property by connecting the secondary mass to a different floor/location from the one that the TMD is attached to. Meanwhile, several inerter prototypes relying on different technologies have been devised and experimentally verified demonstrating that inertance scales-up practically independently from the inerter physical mass (Smith 2020). In this regard, numerous studies focused on the use of TMDI for seismic lateral sway demands mitigation of base-isolated structures and demonstrated the TMDI superiority over the TMD by connecting the secondary mass to the ground via an inerter, numerically (e.g. De Domenico and Ricciardi 2018b, De Angelis et al. 2019) and experimentally (e.g. Pietrosanti et al. 2021). Similarly, several works explored the potential of TMDI for the seismic response mitigation of fixed-based buildings by placing a TMDI towards the top floors (e.g. Giaralis and Taflanidis 2018, Ruiz et al. 2018, Taflanidis et al. 2019, Kaveh et al. 2020, Patsialis et al. 2021, Djerouni et al. 2022). In these studies, it was found that the efficacy of TMDI for seismic response mitigation is considerably enhanced by letting the inerter connect the secondary mass to several floors below the one that the mass is attached to. However, the practicality of TMDI configurations spanning several floors is limited.

To this end, Sedhain and Giaralis (2019) and Wang and Giaralis (2021) recently demonstrated that a TMDI configuration contained within a flexible top storey becomes similarly effective as TMDI configurations spanning several regular floors. In the last works, the flexible storey was materialized by local modifications (e.g., increasing the floor height or reducing the columns sections). Inspired by the above work, this study investigates the possibility of coupling a TMDI with a seismically isolated floor which can be added atop of existing building structures or included in the design of new structures. In this configuration, once the isolators yield under severe ground motion, a flexible top floor is created which, in turn, increases the effectiveness of the TMDI for seismic energy dissipation. The herein configuration termed, rooftop isolated tuned mass damper inerter, (RI-TMDI) resembles the roof-garden partial isolated TMD advocated in Matta and De Stefano (2009), but considers an inerter to reduce significantly the secondary mass. The RI-TMDI is also well-related to TMDI-equipped base isolated structures studied by Domenico and Ricciardi (2018b) and De Angelis et al. (2019) among several other researchers. However, in the aforementioned works, the inerter was grounded while the isolation layer was part of the primary structure to be seismically protected. Instead, in the RI-TMDI the isolation layer is part of the hybrid vibration absorber and is used to improve the efficacy of the TMDI. In the following section, the proposed RI-TMDI is presented and is analytically modelled through a nonlinear dynamical system. Next, optimal RI-TMDI tuning is undertaken based on a energy-based criterion and facilitated by treating the nonlinear term contributed by the isolator through statistical linearization. The optimal tuning and performance of the RI-TMDI is assessed through a parametric numerical investigation assuming white noise seismic excitation, as well as through nonlinear time-history analyses for a small suite of recorded ground motions.

## **PROPOSED ROOFTOP ISOLATED TUNED MASS DAMPER INERTER (RI-TMDI) SYSTEM**

### **System description and mechanical modelling**

The proposed hybrid energy dissipation system is applicable for the seismic protection of existing as well as of new buildings (primary structures). It comprises a seismically isolated rigid slab, placed atop of the primary building structure, and a tuned mass damper inerter (TMDI) sandwiched between the isolated slab and the top-most slab of the primary structure. The resulting rooftop isolated tuned mass damper inerter (RI-TMDI) system is graphically shown in Fig. 1a. From a practical viewpoint, the isolated slab can serve as a roof-garden to a new or to an existing building as demonstrated in Matta and De Stefano (2009). Further, any standard type of isolation bearing used in base isolated buildings may be employed in the RI-TMDI (Naeim and Kelly 1999), though this study adopts lead rubber bearings (LRBs). Moreover, the TMDI can be readily integrated within the isolation layer as it is lightweight and can be made sufficiently compact (see e.g. Pietrosanti et al 2021 and references therein). Specifically, the TMDI (Marian and Giaralis 2013, 2014) consists of a relatively small secondary vibrating mass which is connected to the isolated slab through stiffeners and standard viscous energy dissipative devices (eg. fluid viscous dampers), as shown in Fig.1(b), and to the top-most slab of the primary structure through an inerter device (Smith 2002, 2020). Various compact and lightweight full-scale inerter prototypes with inertance values several orders larger than their physical mass have been devised and

experimentally verified for large-scale structural earthquake engineering applications (e.g. Nakamura et al 2014, Nakaminami et al 2017).

In this work, a simplified mechanical model with three degrees of freedom (3-DOF) is adopted to study the performance of RI-TMDI, shown in Fig. 1b. In this model, the primary structure is represented by a linear damped single degree of freedom structure with mass  $m_s$ , inherent damping coefficient  $c_s$  and stiffness  $k_s$ . The nonlinear behaviour of the LRBs is modelled using the versatile Bouc-Wen hysteretic model (Wen 1980), while  $m_i$  is mass of the isolated slab. Further, a linear TMDI is taken as it has been recently established through pertinent shaking table testing that nonlinear effects do not significantly compromise the motion control efficacy of the TMDI (Pietrosanti *et al.* 2020, 2021). In detail, the TMDI model includes the secondary mass  $m_d$ , the stiffness coefficient  $k_d$ , the viscous damping coefficient  $c_d$ , and the inertance  $b$  (Fig. 1b).

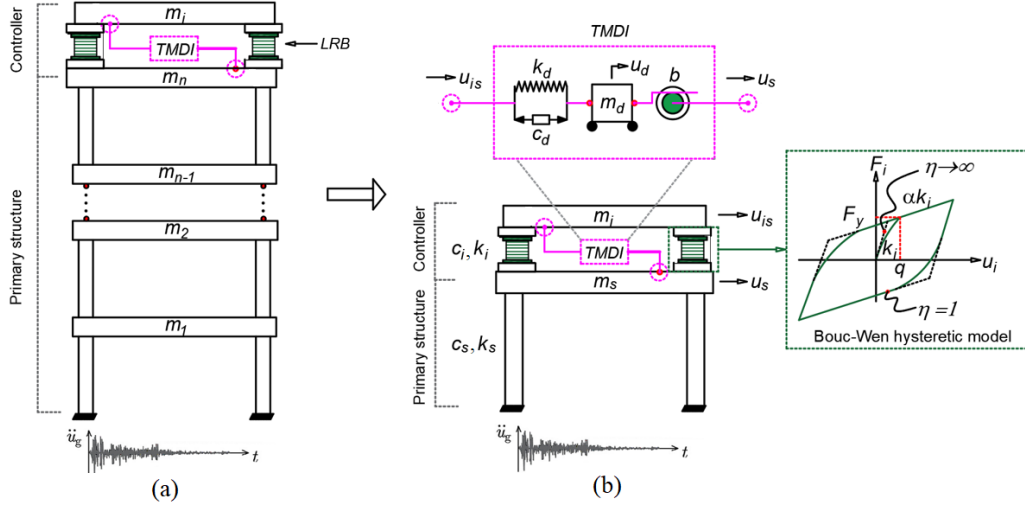


**Figure 1.** Proposed rooftop isolated tuned mass damper inerter (RI-TMDI) system and simplified 3-DOF model of a SDOF primary structure equipped with RI-TMDI

### Nonlinear equations of motion

The governing equations of motion of the 3-DOF mechanical model in Fig.1b under seismic horizontal acceleration excitation  $\ddot{u}_g$  can be written as

$$\begin{aligned}
 m_s \ddot{u}_s + c_s \dot{u}_s + k_s u_s - F_i - F_b &= -m_s \ddot{u}_g \\
 m_i (\ddot{u}_i + \ddot{u}_s) + F_i - c_d \dot{u}_k - k_d u_k &= -m_i \ddot{u}_g \\
 m_d (\ddot{u}_k + \ddot{u}_i + \ddot{u}_s) + c_d \dot{u}_k + k_d u_k + F_b &= -m_d \ddot{u}_g
 \end{aligned} \tag{1}$$

in terms of the relative displacement coordinates  $u_s$ ,  $u_i = u_{is} - u_s$  and  $u_k = u_d - u_{is}$  where  $u_s$ ,  $u_{is}$  and  $u_d$  are the lateral displacements of the primary structure, the isolated slab, and the secondary mass, respectively, relative to the ground. In Eq.(1) and hereafter a dot over a symbol denotes time differentiation. Further,  $F_b$  and  $F_i$  are the restoring forces of the inerter and the LRB. For an ideal linear inerter element, the inerter force is given as (Smith 2002)

$$F_b = b(\ddot{u}_i + \ddot{u}_k), \tag{2}$$

while the LRB force is taken equal to

$$F_i = c_i \dot{u}_i + \alpha k_i u_i + (1 - \alpha) F_y z, \tag{3}$$

where  $c_i$  is the LRB viscous damping coefficient,  $k_i$  is the initial (pre-yielding) LRB lateral stiffness,  $\alpha$  is the rigidity ratio defined as the post-yielding to the pre-yielding LRB stiffness,  $F_y$  is the LRB yielding strength, and  $z$  is a hysteretic coordinate governed by the first-order differential equation (Wen 1976)

$$q\dot{z} = A\dot{u}_i - \gamma|\dot{u}_i|z|z|^{\eta-1} - \beta\dot{u}_i|z|^{\eta}. \quad (4)$$

In the last equation,  $q$  is the LRB yielding displacement, while  $A$ ,  $\beta$ ,  $\gamma$  and  $\eta$  are dimensionless parameters of the Bouc-Wen model which control the shape of the hysteretic loops. By introducing the following dimensionless parameters: natural frequencies of the structure,  $\omega_s$ , and of the TMDI,  $\omega_d$ , as

$$\omega_s = \sqrt{\frac{k_s}{m_s}}, \quad \omega_d = \sqrt{\frac{k_d}{b+m_d}}, \quad (5)$$

critical damping ratios of the structure,  $\xi_s$ , of the LRB,  $\xi_i$ , and of the TMDI,  $\xi_d$ , as

$$\xi_s = \frac{c_s}{2m_s\omega_s}, \quad \xi_i = \frac{c_i}{2\omega_i m_i}, \quad \xi_d = \frac{c_d}{2(m_d+b)\omega_d}, \quad (6)$$

mass ratios of the isolated slab,  $\mu_i$ , and of the TMDI,  $\mu_d$ , and TMDI inertance ratio,  $\beta_d$ , as

$$\mu_d = \frac{m_d}{m_s}, \quad \mu_i = \frac{m_i}{m_s}, \quad \beta_d = \frac{b}{m_s}, \quad (7)$$

and normalized LRB yielding strength,  $F_o$ , as

$$F_o = \frac{F_y}{m_i g}, \quad (8)$$

where  $g=9.81\text{m/s}^2$ , the equations of motion in Eq.(1) can be written in matrix form as

$$\mathbf{M}\ddot{\mathbf{u}} + \mathbf{C}\dot{\mathbf{u}} + \mathbf{K}\mathbf{u} + \mathbf{P}\mathbf{z} = -\delta\ddot{u}_g, \quad (9)$$

where

$$\mathbf{M} = \begin{bmatrix} 1 & -\beta_d & -\beta_d \\ \mu_i & \mu_i & 0 \\ \mu_d & \mu_d + \beta_d & \mu_d + \beta_d \end{bmatrix}, \quad \mathbf{C} = \begin{bmatrix} 2\xi_s\omega_s & -2\xi_i\omega_i & 0 \\ 0 & 2\xi_i\omega_i & -2\xi_d\omega_d(\mu_d + \beta_d) \\ 0 & 0 & 2\xi_d\omega_d(\mu_d + \beta_d) \end{bmatrix}, \quad (10)$$

$$\mathbf{K} = \begin{bmatrix} \omega_s^2 & -\alpha\mu_i\omega_i^2 & 0 \\ 0 & \alpha\mu_i\omega_i^2 & -\omega_d^2(\mu_d + \beta_d) \\ 0 & 0 & \omega_d^2(\mu_d + \beta_d) \end{bmatrix}, \quad \mathbf{P} = \begin{bmatrix} -\mu_i(1-\alpha)F_o g \\ \mu_i(1-\alpha)F_o g \\ 0 \end{bmatrix}, \quad \delta = \begin{bmatrix} 1 \\ \mu_i \\ \mu_d \end{bmatrix}, \quad \mathbf{u} = \begin{bmatrix} u_s \\ u_i \\ u_k \end{bmatrix}$$

It is important to recognize that the system of equations in Eq.(9) is nonlinear due to the hysteretic generalized coordinate  $z$  in Eq.(4). This nonlinearity significantly impedes the design/tuning of RI-TMDI by requiring computationally expensive nonlinear response history analyses. To this end, RI-TMDI design is herein expedited by assuming that the seismic excitation is a Gaussian stationary random process and by treating the nonlinear relationship in Eq.(4) through statistical linearization to define an equivalent linear stochastically excited system. The response statistics of the equivalent linear system are then used for optimal RI-TMDI tuning. The next section presents the statistical linearization step and response statistics derivation for the equivalent linear system.

## STATISTICAL LINEARIZATION AND RANDOM VIBRATION ANALYSIS

The statistical linearization scheme proposed by Wen (1980) replaces the nonlinear first-order differential equation in Eq.(4) by the following linear equation

$$qz = -c_{eq}\dot{x}_i - k_{eq}z, \quad (11)$$

where  $c_{eq}$  and  $k_{eq}$  are deterministic parameters. Under the assumption of  $\ddot{u}_g$  being a stationary Gaussian stochastic process and taking  $z$  and  $\dot{x}_i$  processes in Eq.(11) to be jointly Gaussian, the parameters  $c_{eq}$  and  $k_{eq}$  can be determined in closed form by minimising the expected value of the squared difference between the right hand side of Eq.(4) and Eq.(11) (see also Roberts and Spanos 2003 and Mitseas et al 2018). For the special case of  $\eta=1$ , which defines smooth hysteretic loops, the parameters  $c_{eq}$  and  $k_{eq}$  are found by (Wen 1980)

$$c_{eq} = \sqrt{\frac{2}{\pi}} \left( \gamma \frac{E[\dot{x}_i z]}{\sigma_{\dot{x}_i}} + \beta \sigma_z \right) - A, \quad k_{eq} = \sqrt{\frac{2}{\pi}} \left( \gamma \sigma_{\dot{x}_i} + \beta \frac{E[\dot{x}_i z]}{\sigma_z} \right), \quad (12)$$

where  $E[.]$  is the mathematical expectation operator and  $\sigma_z$  and  $\sigma_{\dot{x}_i}$  are the standard deviation of the processes  $z$  and  $\dot{x}_i$ , respectively.

To this end, the equations of motion of the nonlinear RI-TMDI equipped SDOF system in Eqs.(4) and (10) are approximated by a surrogate linear system of equations corresponding to an equivalent linear structural system (ELS). The equations of motion of the ELS are written in state-space form as

$$\dot{\mathbf{x}} = \mathbf{A}\mathbf{x} + \mathbf{B}\ddot{u}_g, \quad (13)$$

where

$$\mathbf{A} = \begin{bmatrix} \mathbf{0}_{(3,3)} & \mathbf{I}_{(3)} & \mathbf{0}_{(3,1)} \\ -\mathbf{M}^{-1}\mathbf{K} & -\mathbf{M}^{-1}\mathbf{C} & -\mathbf{M}^{-1}\mathbf{P} \\ \mathbf{0}_{(1,3)} & \left\{ 0 \quad -\frac{c_{eq}}{q} \quad 0 \right\} & -\frac{k_{eq}}{q} \end{bmatrix}, \quad \mathbf{B} = \begin{bmatrix} 0 \\ 0 \\ 0 \\ 1 \\ 1 \\ 1 \\ 0 \end{bmatrix}, \quad \mathbf{x} = \begin{bmatrix} x_s \\ x_i \\ x_k \\ \dot{x}_s \\ \dot{x}_i \\ \dot{x}_k \\ z \end{bmatrix}. \quad (14)$$

In the above expressions,  $\mathbf{0}_{(m,n)}$  is the m-by-n zero matrix,  $\mathbf{I}_{(m)}$  is the m-by-m identity matrix, and the exponent (-1) demotes matrix inversion. Note that in Eqs.(13) and (14) the response displacement coordinates of the ELS are denoted by a different symbol from those of the nonlinear system in Eqs. (4) and (10) (i.e.  $x$  is used instead of  $u$ ) to emphasize that the ELS response is an approximation of the response of the nonlinear system. Importantly, the parameters  $c_{eq}$  and  $k_{eq}$  in Eq.(12) depend on the ELS response statistics of  $z$  and  $\dot{x}_i$ . For the case of  $\ddot{u}_g$  being Gaussian white noise, the response statistics of the ELS populating the covariance matrix  $\mathbf{\Gamma}$  are found by solving the Lyapunov equation (e.g. Roberts and Spanos 2003)

$$\mathbf{A}\mathbf{\Gamma} + \mathbf{\Gamma}\mathbf{A}^T + 2\pi S_o \mathbf{B}\mathbf{B}^T = 0 \quad (15)$$

where  $S_o$  is the spectral intensity of the white noise. In this work, the white noise ground acceleration intensity is related to the peak ground acceleration (PGA) using the expression

$$S_o = \frac{\text{PGA}^2}{9\omega_{max}} \quad (16)$$

which is derived based on a 3-sigma rule assumption between standard deviation and peak value. In Eq.(16)  $\omega_{max}$  is the maximum excitation frequency taken equal to  $20\pi$  rad/s.

In the ensuing computational work, the Lyapunov equation in Eq.(15) is numerically solved using the built-in MATLAB function `lyap` to obtain the covariance matrix  $\mathbf{\Gamma}$ . The diagonal elements of the covariance matrix are the variances of all the states in vector  $\mathbf{x}$ , while the off-diagonal elements include all the response cross-

variance terms. Given dimensionless parameters in Eqs.(5)-(8) and the white noise intensity in Eq.(16), the parameters  $c_{eq}$  and  $k_{eq}$  of the ELS in Eq.(12) and the ELS response statistics in  $\Gamma$  are determined numerically by iterative use of Eqs. (12) and (15) until convergence (i.e. until the change of the parameters are below a pre-defined threshold) as detailed in Roberts and Spanos (2003).

## ENERGY-BASED OPTIMAL DESIGN OF THE RI-TMDI

The optimal RI-TMDI design/tuning scheme adopted in this study treats the TMDI stiffness and damping properties as the primary (free) design variables, while the remaining RI-TMDI properties are taken as secondary (fixed). This consideration facilitates the parametric investigation of the RI-TMDI performance for different LRB and inerter properties which are expected to be critical for the seismic performance of the 3-DOF system in Fig. 1b based on previous works (De Domenico and Ricciardi 2018, De Angelis et al. 2019, Wang and Giaralis 2021). The objective function of the optimal design problem to be minimized is taken to be the so-called filtered energy index (FEI) (De Domenico and Ricciardi 2018a, 2018b) defined as

$$FEI = 1 - \frac{c_d \sigma_{\dot{x}_k}^2}{c_s \sigma_{\dot{x}_s}^2 + c_d \sigma_{\dot{x}_k}^2 + c_b \sigma_{\dot{x}_i}^2 + (1-\alpha) F_y \sigma_{\dot{x}_{iz}}}. \quad (17)$$

The above energy performance function stems from the work of Reggio and De Angelis (2015) and represents the portion of the total input seismic energy which is not dissipated by the damping element of the TMDI, thus stressing the LRB and the primary structure (see also De Angelis et al. 2019). By minimizing FEI in Eq.(17), the energy dissipated by the TMDI is maximized (numerator in the right hand side ratio of Eq.(17)) which ultimately protects the primary structure and reduces the deflection of the LRBs.

In this setting, the optimization problem governing the design of the RI-TMDI is defined as: find the TMDI stiffness and damping properties which minimize FEI in Eq.(17) given the primary structure properties, LRB properties and TMDI inertial (mass and inertance) properties under white noise excitation with  $S_o$  spectral intensity. This is mathematically written as

$$\min_{\mathbf{y}_1} \{FEI | \mathbf{y}_2\}, \quad (18)$$

where  $\mathbf{y}_1 = \{\zeta_d \lambda\}$  with  $\lambda = \omega_d / \omega_s$  is the vector of the primary nondimensional design variables and  $\mathbf{y}_2 = \{\omega_s \zeta_s \zeta_i \mu_i \mu_d \beta_d F_o\}$  is the vector of the secondary design variables. Notably, with  $\zeta_d$  and  $\lambda$  known, the TMDI stiffness and damping properties  $k_d$  and  $c_d$  can be found from Eqs. (5) and (6). The optimization problem in Eq.(18) is solved numerically using a pattern search algorithm implemented in the built-in MATLAB function `fminsearch`. The solution requires evaluation of all the ELS response statistics appearing in Eq.(17) which are contained in the covariance matrix  $\Gamma$  found by solving Eq.(15) as part of the statistical linearization.

## PARAMETRIC INVESTIGATION OF OPTIMAL RI-TMDI TUNING AND ELS PERFORMANCE

In this section optimal RI-TMDI tuning is pursued under white noise excitation for a range of different LRB and inertance properties, while performance is gauged with respect to the ELS displacement variance of the primary structure and of the isolated slab, and  $\sigma_{x_s}$  and  $\sigma_{x_i}$ , respectively. In all structural systems considered in this parametric investigation, the primary structure inherent damping ratio and natural frequency are taken as  $\xi_s = 0.01$  and  $\omega_s = 2\pi$  (i.e. natural period 1s), respectively. The Bouc-Wen model parameters are taken as  $A=1$ ,  $\beta=\gamma=0.5$  and  $\eta=1$ , commonly assumed in the literature to represent LRBs with smooth strain-softening behavior (Jangid 2010, De Domenico and Ricciardi 2018b). The mass ratio of the isolated slab is taken as  $\mu_i = 0.10$  to roughly correspond to the mass of one story in a 10-storey primary building structure. A small TMDI secondary mass ratio is chosen as  $\mu_d = 0.01$  to account for the physical mass of the TMDI device equipment and connections. A wide range of inertance ratios  $\beta_d$  from 0.5% to 25% is considered in the parametric investigation. Note that such inertance ratios are foreseen to be technologically realizable for most building structures, based on the scalability of full-scale inerter prototypes that have been experimentally verified in the literature. For instance, the ball-screw inerter prototype in Nakamura et al. (2014) reached 2000t of inertance,

while the hydraulic inerter prototype in Nakaminami et al. (2017) exceeded 10000t of inertance. Further, different values of the LRB viscous damping ratio  $\xi_i$  and normalized yielding strength,  $F_o$ , are considered to study the influence of the LRB damping and effective flexibility. The latter is herein quantified through the effective post-yield isolation period defined as (e.g. Jangid 2010)

$$T_i = 2\pi \sqrt{\frac{m_i}{\alpha k_i}} = 2\pi \sqrt{\left( \frac{q}{F_o g \alpha} \right)}. \quad (19)$$

In this work, the LRB yielding displacement is kept constant at  $q=0.015$  m and the rigidity ratio is taken equal to  $\alpha=0.1$ . Therefore, by the varying the normalized yielding strength, the effective LRB period  $T_i$  in Eq.(19) changes to model LRBs with different effective flexibility. This is key consideration for the RI-TMDI as previous work (Sedhain and Giaralis 2019, Wang and Giaralis 2021) have shown that TMDI motion mitigation effectiveness improves as the flexibility of the storey the TMDI is installed to increases. In all cases, a PGA value of 0.3g is assumed in specifying the white noise excitation intensity in Eq.(16).

### Influence of LRB effective flexibility with inertance

Figure 2 reports results from optimal RI-TMDI designs obtained by solving Eq.(18). Specifically, the objective function (FEI) and the optimal TMDI tuning parameters are plotted against the inertance ratio  $\beta_d$  for 5 different values of LRB normalised yielding strength  $F_o$ . The corresponding isolation period in Eq.(19) is included in the Fig.2 for the different  $F_o$  values. The LRB viscous damping ratio is taken equal to  $\xi_i = 0.01$  which is a commonly adopted value for LRBs (De Domenico and Ricciardi 2018b).

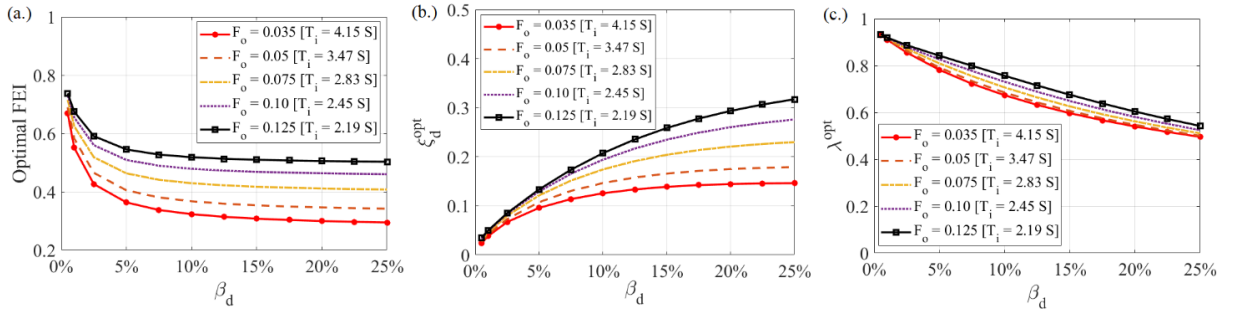


**Figure 2.** (a) Objective function (FEI), (b) optimal TMDI viscous damping ratio and (c) optimal TMDI frequency ratio plotted against inertance ratio, for five different LRB yielding strength values  $F_o$ .

It is seen, Fig. 2a, that FEI decreases monotonically with the inertance for all considered LRBs verifying the key role of inertance to increase seismic energy dissipation at the TMDI rather than at the LRBs. This is achieved through an increase to the optimal TMDI damping property as seen in Fig 2b. Nevertheless, the rate of FEI decrease with inertance saturates rapidly and increase of  $\beta_d$  above 8% has insignificant effect to FEI. More importantly, FEI reduces significantly for any fixed inertance value as the LRB effective flexibility increases (i.e. as the LRB normalised yielding strength  $F_o$  reduces). This is an important outcome which confirms the engineering intuition behind employing isolation bearings to enable a soft top-floor which, in turn, improves the motion control efficacy of TMDI as demonstrated in recent publications (Sedhain and Giaralis 2019, Wang and Giaralis 2021). Caution needs to be exercised, however, to ensure that sufficient inertance is provided to the TMDI (at least 5% inertance ratio for the case-study herein considered) as for small inerter values, large FEI values are noted, indicating that seismic energy dissipation takes place at the LRBs, rather than at the TMDI. Regarding the optimal TMDI tuning ratio  $\lambda = \omega_d / \omega_s$ , it is seen in Fig. 2c that it depends and varies more with inertance, rather than with LRB flexibility, which is the opposite compared to the optimal TMDI damping ratio in Fig. 2b.

The effectiveness of the optimal RI-TMDI tuning in Fig.2 is assessed in Fig.3 by plotting the ELS displacement variance of the primary structure and of the isolated floor versus the inertance ratio and for the five different LRB yielding strength values. Results are normalized by the uncontrolled structure displacement variance  $\sigma_{x_o}^2$  of the primary structure exposed to the same white noise excitation. Interestingly, the trends of primary structure variance in Fig. 3a with inertance follow those of FEI in Fig.2a only for the more flexible LRBs. For

LRBs with isolation period  $T_i$  below 2.5s, an increase in the inertance ratio above 3% results in increasing the response of the RI-TMDI equipped primary structure. Still, for any fixed value of inertance above 3%, significant reductions to the primary structure response are achieved by reducing the LRB isolation period. Nevertheless, these improvements come at the cost of increased isolator deflections as shown in Fig.3b. Conveniently, though, Fig. 3b also suggests that the isolator deflections are effectively reduced by increasing the inertance. Overall, the reported data in Fig. 3 demonstrate that there are non-trivial dependencies between inertance, LRB flexibility, primary structure vibration mitigation and isolator deflections. In this regard, careful RI-TMDI design is required which should employ sufficiently flexible LRBs for improved vibrations mitigation of the primary structure in conjunction with sufficiently large inertance values (10% or above for the case-study) to ensure that vibration mitigation is driven by the TMDI and not by the LRBs while LRB seismic deflection demands remain at reasonable levels, comparable with the deflection of the uncontrolled primary structure.

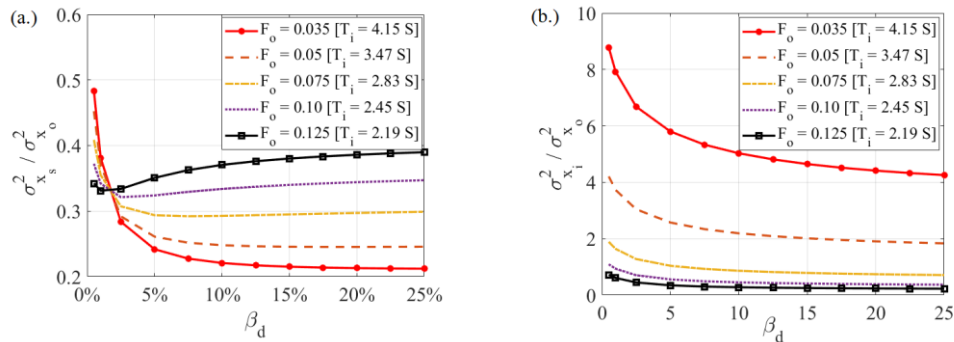


**Figure 3.** Normalized displacement variance of (a) primary structure and (b) isolated slab by the displacement variance of the uncontrolled primary structure  $\sigma_{x_0}^2$  versus inertance ratio for various  $F_o$ .

### Influence of LRB viscous damping with inertance

Herein, attention is turned to quantifying the influence of the LRB viscous damping ratio  $\xi_i$  to the optimal RI-TMDI tuning and performance. To this aim, Fig.4 plots FEI and optimal TMDI tuning parameters against the inertance ratio  $\beta_d$  for three different values of  $\xi_i$ , while Fig.5 plots *ELS* displacement variance of the primary structure and of the isolated floor versus the inertance ratio for the same  $\xi_i$  values. A common normalised LRB yielding strength  $F_o = 0.075$  is assumed. The range of  $\xi_i$  values considered are based on previous published literature on LRB modelling through the Bouc-Wen model (Jangid 2010, De Domenico and Ricciardi 2018b) and represent different levels of rubber damping properties. It is found that the optimal TMDI tuning parameters are relatively insensitive to  $\xi_i$ , especially for inertance ratios up to 10% (Fig. 4). Still,  $\xi_i$  significantly affects the deflection of the primary structure and of the isolated layer for any fixed inertance value as seen in Fig. 5. Lower value of  $\xi_i$  is beneficial to the primary structure response, but it is detrimental to the deflection of the isolators. In this respect, the selection of  $\xi_i$  is an important design parameter in the RI-TMDI, together with the inertance and the LRB flexibility which needs to be carefully decided upon to leverage the trade-off between primary structure and isolation layer deflections.

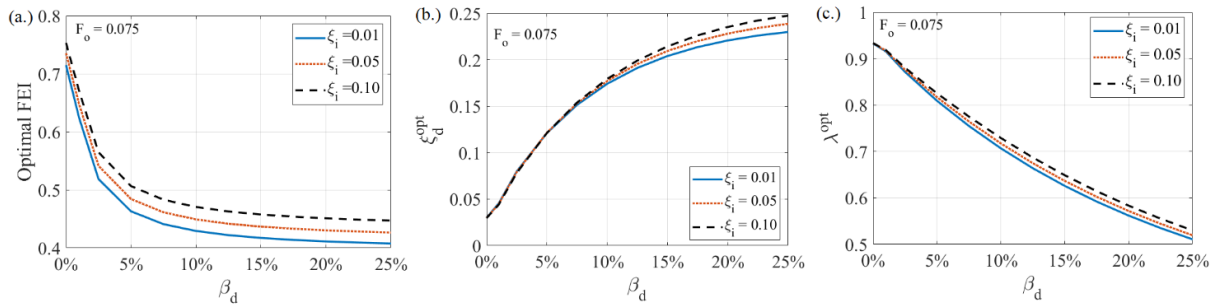


**Figure 4.** (a) Objective function (FEI), (b) optimal TMDI viscous damping ratio and (c) optimal TMDI frequency ratio plotted against inertance ratio, for three different LRB critical damping ratio values  $\xi_i$ .

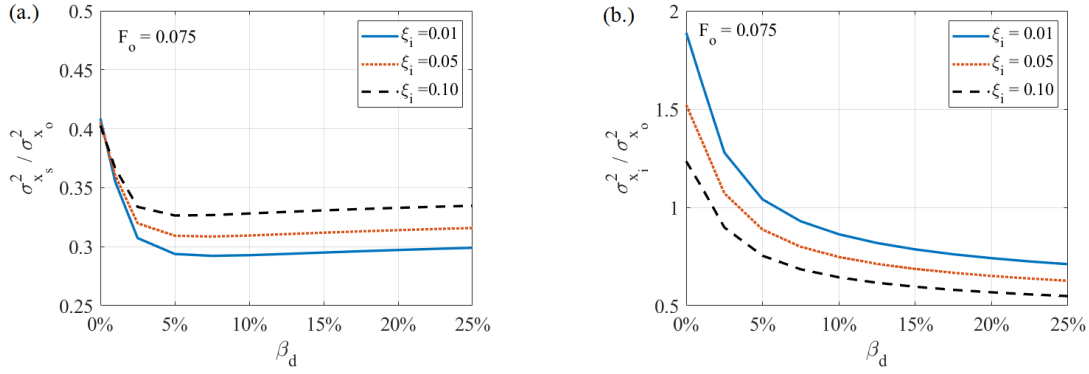


**Figure 5.** Normalized displacement variance of (a) primary structure and (b) isolated slab by the displacement variance of the uncontrolled primary structure  $\sigma_{x_o}^2$  versus inertance ratio for various  $\xi_i$ .

## SEISMIC PERFORMANCE ASSESSMENT OF OPTIMAL RI-TMDI EQUIPPED STRUCTURES

In the previous section, white noise excitation was assumed to model the seismic action while performance was gauged using the ELS. Nevertheless, earthquake-induced ground motion has time-varying amplitude and frequency content, while the ELS is an approximation of the nonlinear RI-TMDI system in Fig.1b. Therefore, it is deemed essential to assess the seismic performance of the RI-TMDI using nonlinear response history analysis (NRHA) for a number of field-recorded earthquake ground motions (GMs). In this regard, two near-field and two far-field GMs are considered which have been adopted by Ohtori et al (2004) for benchmark seismic assessment of buildings equipped with vibration control devices. The far-field records have been recorded during the El Centro event (1940) and the Tokachi-ochi event (1968) with PGA  $3.417 \text{ m/s}^2$  and  $2.250 \text{ m/s}^2$ , respectively. The near-field records have been recorded during the Northridge event (1994) and the Kobe event (1995) with PGA  $8.2676 \text{ m/s}^2$  and  $8.1782 \text{ m/s}^2$ , respectively. Fig. 6 plots primary structure displacement time-histories obtained from NRHA for two different RI-TMDI systems, optimally tuned for white noise excitation as detailed in the previous section. The four GMs are scaled such that their PGA becomes equal to  $0.3g$  which was assumed in the optimal RI-TMDI tuning. This scaling is deemed essential to ensure consistency of the seismic action intensity used for RI-TMDI design and assessment. To draw an interesting comparison, one system has the stiffest LRB properties of those considered in the previous section ( $F_o = 0.125$ ;  $T_i = 2.19\text{s}$ ) and the other system has the most flexible LRB properties ( $F_o = 0.035$ ;  $T_i = 4.15\text{s}$ ).

It is found that RI-TMDI reduces appreciably the peak and, even more, the root mean square response of the primary structure for all four considered GMs compared to the uncontrolled structure. It is also seen that the RI-TMDI system with the most flexible LRBs is significantly more effective than the system with the stiffer LRBs for all the GMs. Overall, the reported time-history data from NRHA confirm the trends in Fig. 3a, which used the ELS response under white noise excitation, and establish the potential of RI-TMDI for seismic protection of building structures.

## CONCLUDING REMARKS

This paper presented a novel hybrid energy dissipation system for the seismic protection of buildings, termed RI-TMDI, which combines an additional “fake” seismic isolated floor with a TMDI placed atop building structures. The motivation of the RI-TMDI was based on the fact that the vibration control potential of TMDIs improve as the floor they are installed to is designed to be more flexible. A 3-DOF structural system has been put forward to study the potential of RI-TMDI for the task in which isolator bearings have been modelled through the Bouc-Wen model. Statistical linearization was applied to expedite optimal RI-TMDI tuning such that the input energy dissipated by the TMDI is maximized under white noise excitation. A pilot parametric numerical investigation was undertaken to assess the influence of the isolator flexibility and damping properties, taken as LRBs, and of the TMDI inertance to the tuning and performance of the RI-TMDI under white noise excitation. Further, NRHA results for four recorded GMs applied to two different optimally tuned RI-TMDI systems were reported.

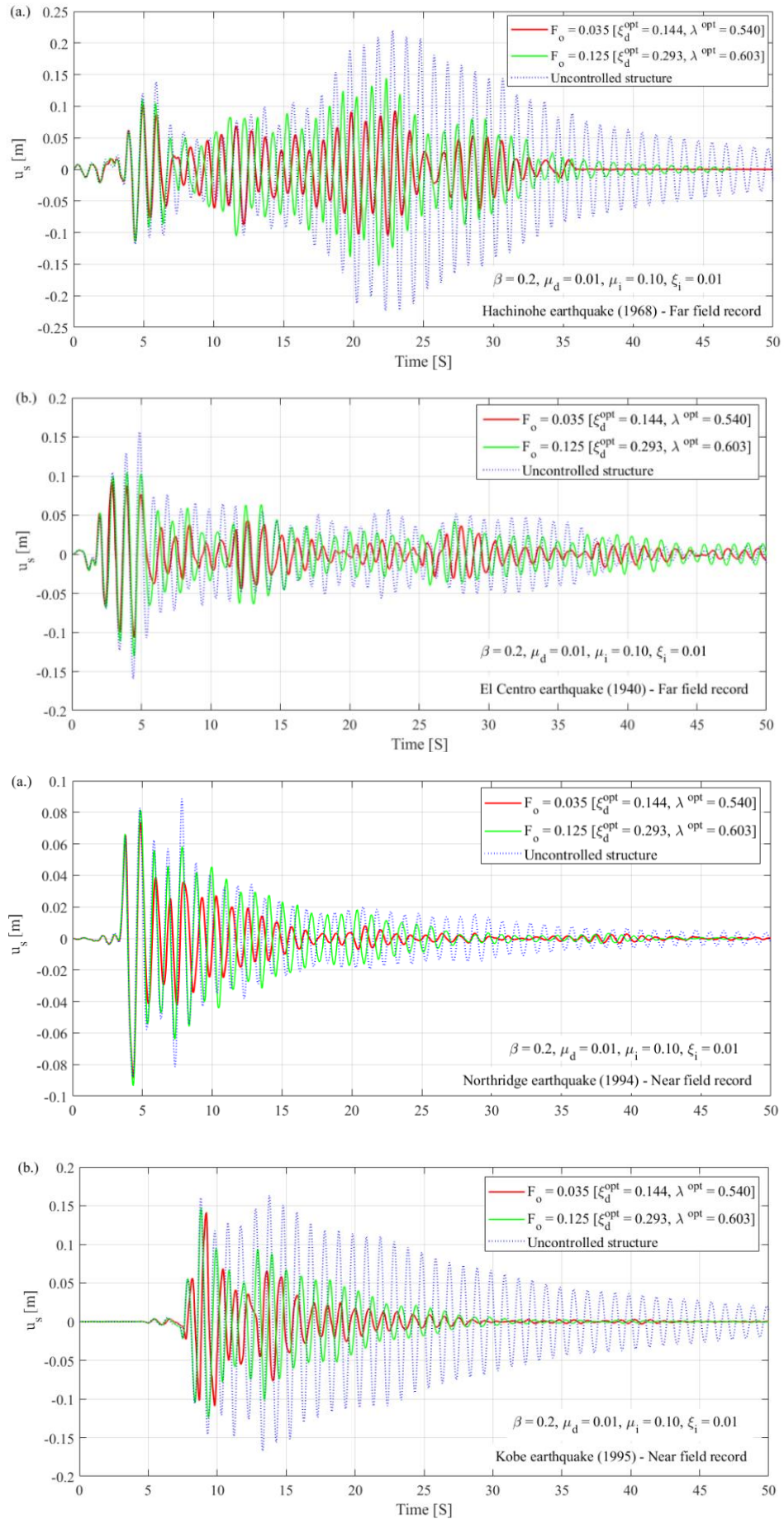


**Figure 6.** Primary structure response of uncontrolled and RI-TMDI equipped structures under different recorded ground motions obtained by response history analysis.

The overarching finding from the herein reported numerical results is that there is a trade-off between the building structure displacement demand and the deflection of the isolators. In detail, the efficacy of RI-TMDI for suppressing seismic structural displacement demands improves as the effective post-yielding flexibility of the LRB isolators increases, provided that the TMDI is equipped with sufficiently high inertance. This effect has been demonstrated for both white noise excitation and for recorded GMs. However, this improvement comes at the cost of increased deflection of the isolators. These deflections may be contained by increasing the viscous damping property in the LRB isolators, which, nevertheless, is detrimental to building structure response, as shown under white noise excitation. Still, by increasing inertance and using flexible LRBs, both building and isolator displacements are reduced under white noise excitation.

Overall, numerical results presented in this pilot study demonstrate good potential of RI-TMDI for seismic retrofitting existing building structures as well as for improving the seismic performance of new ones. However, further work is warranted to explore the trade-off between inertance and isolator flexibility for different structural properties, levels of seismic intensity and types of isolators. Extension to the case of multi-storey building models is further left for future work.

## REFERENCES

- De Angelis M., Perno S., Reggio A. (2012). Dynamic response and optimal design of structures with large mass ratio TMD. *Earthquake Engineering and Structural Dynamics*, 41, pp. 41-60.
- De Angelis M., Giaralis A., Petrini F., Pietrosanti D. (2019). Optimal tuning and assessment of inertial dampers with grounded inerter for vibration control of seismically excited base-isolated systems. *Engineering Structures*, 196, 109250.
- De Domenico D., Ricciardi G. (2018a). Earthquake-resilient design of base isolated buildings with TMD at basement: Application to a case study. *Soil Dynamics and Earthquake Engineering*, 113, pp. 503-521.
- De Domenico D., Ricciardi G. (2018b). Optimal design and seismic performance of tuned mass damper inerter (TMDI) for structures with nonlinear base isolation systems. *Earthquake Engineering and Structural Dynamics*, 47, pp.2539-2560.
- Djerouni S., Ounis A., Elias S., Adbeddaim M., Rupakhety R. (2022). Optimization and performance assessment of tuned mass damper inerter systems for control of buildings subjected to pulse-like ground motions. *Structures*, 38, pp. 139-156.
- Giaralis A., Taflanidis A.A. (2018). Optimal tuned mass-damper-inerter (TMDI) design for seismically excited MDOF structures with model uncertainties based on reliability criteria. *Structural Control and Health Monitoring*, 25, e2082.
- Jangid R., (2010). Stochastic response of building frames isolated by lead-rubber bearings. *Structural Control and Health Monitoring*, 17, pp.1-22.
- Kaveh A., Farzam M.F., Jalali H.H. (2020). Statistical seismic performance assessment of tuned mass damper inerter. *Structural Control and Health Monitoring*, 27, e2602.
- Marian L., Giaralis A. (2013). Optimal design of inerter devices combined with TMDs for vibration control of buildings exposed to stochastic seismic excitations. 11<sup>th</sup> International Conference on Structural Safety and Reliability for Integrating Structural Analysis, Risk and Reliability, paper #137, pp. 1025-1032.
- Marian L., and Giaralis A. (2014). Optimal design of a novel tuned mass-damper-inerter (TMDI) passive vibration control configuration for stochastically support-excited structural systems. *Probabilistic Engineering Mechanics*, 38, pp. 156-164.
- Matta E, De Stefano A. (2009). Seismic performance of pendulum and translational roofgarden TMDs. *Mechanical Systems and Signal Processing*, 23, pp. 908-921.
- Mitseas IP, Kougioumtzoglou IA, Giaralis A and Beer M (2018). A novel stochastic linearization framework for seismic demand estimation of hysteretic MDOF systems subject to linear response spectra. *Structural Safety*, 72: 84-98.
- Naeim F. & Kelly J. (1999). *Design of Seismic Isolated Structures: From Theory to Practice*. Wiley. New York.
- Nakamura, Y., Fukukita, A., Tamura, K., Yamazaki, I., Matsuoka T, Hiramoto K, Sunakoda K. Seismic response control using electromagnetic inertial mass dampers. *Earthquake Engineering & Structural Dynamics* 2014;43(4):507–27.
- Nakaminami, S., Kida, H., Ikago, K., Inoue N. (2017). Dynamic testing of a full-scale hydraulic inerter-damper for the seismic protection of civil structures. 7<sup>th</sup> International conference on advances in experimental structural engineering, (pp. 41–54). DOI: 10.7414/7aese.T1.55.2016.
- Ohtori Y., Christenson R., Spencer B., Dyke S. (2004). Benchmark Control Problems for Seismically Excited Nonlinear Buildings. *Journal of Engineering Mechanics*, 130, pp.366-385.

- Patsialis D., Taflanidis A.A., Giaralis A. (2021). Tuned-mass-damper-inerter optimal design and performance assessment for multi-storey hysteretic buildings under seismic excitation. *Bulletin of Earthquake Engineering*, DOI: 10.1007/s10518-021-01236-4.
- Pietrosanti, D., De Angelis, M. and Giaralis, A. (2020). Experimental shaking table study of nonlinear SDOF system equipped with tuned mass damper inerter (TMDI) under harmonic excitation. *International Journal of Mechanical Sciences*, 184: 105762.
- Pietrosanti D, De Angelis M, Giaralis A. (2021). Experimental seismic performance assessment and numerical modelling of nonlinear inerter vibration absorber (IVA)- equipped base isolated structures tested on shaking table. *Earthquake Engineering and Structural Dynamics*, 50, pp. 2732–53.
- Reggio A., De Angelis M. (2015). Optimal energy-based seismic design of non-conventional tuned mass damper (TMD) implemented via inter-story isolation. *Earthquake Engineering and Structural Dynamics*, 44, pp. 1623-1642.
- Roberts J.B., Spanos P.D. (2003). *Random vibration and statistical linearization*. Dover Publications, Mineola.
- Ruiz R., Taflanidis A.A., Giaralis A. Lopez-Garcia, D. (2018). Risk-informed optimization of the tuned mass-damper-inerter (TMDI) for the seismic protection of multi-storey building structures. *Engineering Structures*, 177, pp.836-850.
- Sedhain S and Giaralis A (2019) Enhanced optimal tuned mass-damper-inerter performance for seismic protection of multi-storey buildings via top-storey softening. In: *SECED 2019 Conference on Earthquake Risk and Engineering Towards a Resilient World* (September 9-10, 2019, Greenwich, UK), pp.10
- Smith M., 2002. Synthesis of mechanical networks: the inerter. *IEEE Transactions on Automatic Control*, 47(10), pp.1648-1662.
- Smith, M. 2020. The inerter: a retrospective. *Annual Reviews in Control, Robotics, and Autonomous Systems*, 3 361-391.
- Taflanidis A.A., Giaralis A. Patsialis D. (2019). Multi-objective optimal design of inerter-based vibration absorbers for earthquake protection of multi-storey building structures. *Journal of the Franklin Institute*, 356, pp. 7754-7784.
- Wang, Z. and Giaralis, A., 2021. Top-Story Softening for Enhanced Mitigation of Vortex Shedding-Induced Vibrations in Wind-Excited Tuned Mass Damper Inerter-Equipped Tall Buildings. *Journal of Structural Engineering*, 147(1), p.04020283.
- Wen Y.K., (1976). Method for random vibration of hysteretic systems. *Journal of the Engineering Mechanics Division ASCE* 102, pp. 249-263.
- Wen Y.K. (1980). Equivalent linearization for hysteretic systems under random excitation. *Journal of Applied Mechanics ASME* 47, pp. 150-154.